

Three-dimensional cell-culture platform based on hydrogel with tunable microenvironmental properties to improve insulin-secreting function of MIN6 cells

Miao Zhang^a, Sen Yan^a, Xueqin Xu^b, Tingting Yu^c, Zhaobin Guo^d, Ming Ma^a, Yi Zhang^e, Zhuxiao Gu^f, Yiwei Feng^b, Chunyue Du^b, Mengqi Wan^b, Ke Hu^{b,*,**}, Xiao Han^{g,***}, Ning Gu^{a,*}

^a State Key Laboratory of Bioelectronics, Jiangsu Key Laboratory for Biomaterials and Devices, School of Biological Sciences and Medical Engineering, Southeast University, Nanjing 210096, China

^b Key Laboratory of Clinical and Medical Engineering, School of Biomedical Engineering and Informatics, Department of Biomedical Engineering, Nanjing Medical University, Nanjing, 211166, Jiangsu, China

^c Department of Medical Genetics, School of Basic Medical Science & Jiangsu Key Laboratory of Xenotransplantation, Nanjing Medical University, Nanjing, 211166, Jiangsu, China

^d Institute for Nanobiotechnology, Johns Hopkins University, Baltimore, MD, USA

^e Department of Colorectal Surgery, The First Affiliated Hospital of Nanjing Medical University, Nanjing, 210029, Jiangsu, China

^f Jiangsu Key Laboratory of Oral Diseases, Department of Prosthodontics, Affiliated Hospital of Stomatology, Nanjing Medical University, Nanjing, 210029, Jiangsu, China

^g Key Laboratory of Human Functional Genomics of Jiangsu Province, Department of Biochemistry and Molecular Biology, Nanjing Medical University, Nanjing, 211166, Jiangsu, China

ARTICLE INFO

Keywords:

3D cell culturing
Hydrogel
Microenvironment
Pancreatic islet β -cells
Insulin secretion

ABSTRACT

Pancreatic β -cells have been reported to be mechanosensitive to cellular microenvironments, and subjecting the cells to more physiologically relevant microenvironments can produce better results than when subjecting them to the conventional two-dimensional (2D) cell-culture conditions. In this work, we propose a novel three-dimensional (3D) strategy for inducing multicellular spheroid formation based on hydrogels with tunable mechanical and interfacial properties. The results indicate that MIN6 cells can sense the substrates and form tightly clustered monolayers or multicellular spheroids on hydrogels with tunable physical properties. Compared to the conventional 2D cell-culture system, the glucose sensitivities of the MIN6 cells cultured in the 3D culture model is enhanced greatly and their insulin content (relative to the amount of protein) is increased 7.3–7.9 folds. Moreover, the relative gene and protein expression levels of some key factors such as Pdx1, NeuroD1, Piezo1, and Rac1 in the MIN6 cells are significantly higher on the 3D platform, compared to the 2D control group. We believe that this 3D cell-culture system developed for the generation of multicellular spheroids will be a promising platform for diabetes treatment in clinical islet transplantation.

1. Introduction

Diabetes, including type 1 and type 2 diabetes, results from the absolute or relative deficiency of insulin [1,2]. Pancreatic β -cell lines such as MIN6 cells or other cell lines are primarily responsible for the regulation of insulin synthesis and secretion, and are, therefore, crucial in systemic glucose homeostasis. Disorders in diabetes include hyperglycemia and hyperlipidemia, which lead to loss of β -cell functionality and

mass, which in turn, worsens the disease [3]. Currently, islet cell transplantation provides a promising therapeutic treatment for patients with diabetes mellitus. However, one of the most challenging problems is low islet survival, especially, the destruction of β cells after islet transplantation, which reduces the insulin storage capacity and glucose-stimulated insulin secretion [4]. This might be due to the disruption of the integrity of the cellular structure and microenvironment. Many approaches have been investigated to improve the quality of

* Corresponding author.

** Corresponding author.

*** Corresponding author.

E-mail addresses: kehu@njmu.edu.cn (K. Hu), hanxiao@njmu.edu.cn (X. Han), guning@seu.edu.cn (N. Gu).

<https://doi.org/10.1016/j.biomaterials.2021.120687>

Received 15 September 2020; Received in revised form 10 December 2020; Accepted 18 January 2021

Available online 21 January 2021

0142-9612/© 2021 Elsevier Ltd. All rights reserved.

β cells and enhance the outcome of islet transplantation techniques such as tissue-engineering strategies. These methods include the encapsulation of islet cells to protect them from the immune response, transplantation of islet cells along with support cells, design of an artificial pancreas, optimization of islet transplant sites, and so on [5–9].

Recently, it was reported that cell behavior as well as cellular functions were strongly influenced by the cellular microenvironments that surrounded them. Pancreatic β cells are mechanosensitive, and their viability and functioning are affected by the local mechanical micro-environment. In particular, the mouse pancreatic β -cell line MIN6 showed increased insulin secretion as well as glucose sensitivity when grown on softer scaffolds than when grown on stiffer scaffolds [10]. These results indicated that a three-dimensional (3D) cell-culture system wherein cells were subjected to a more physiologically relevant micro-environment would be more optimal than the conventional 2D cell culture on planar plates. However, the conventional 3D culture model including 3D multicellular spheroids was established in a microenvironment in which the specificity of islets was lost. For example, the anti-adhesion method is commonly used to establish 3D spheroid models in which cells are cultured in a microenvironment completely deprived of cell adhesion and spheroids are generated by forced aggregation. This method tends to sensitize cells towards necrosis/apoptosis and produces behaviors different from those *in vivo*. Therefore, we propose leveraging the physical factors within microenvironments to induce the formation of multicellular spheroids via self-organization. A recent study published by Mooney's group [11] pointed out that the fates of different cell types were determined by the integration of various physical environmental features in 3D cell culture, such as the stiffness, adhesion ligands, stress relaxation, etc. [12–14]. It had been reported that the stem-cell fate could be determined by the matrix stiffness [15], while the interactions between the cells and extracellular matrix (ECM) played a vital role in regulating the force transmission in certain developmental contexts [14]. The composition and density of adhesion ligands was reported to guide cell adhesion, migration, and polarization [16–18]. Stress relaxation was found to affect the magnitudes of gene expression responses [19].

Previously, we had been working on the development of novel hydrogel materials. By regulating the physical properties of the hydrogel to mimic the ECM, a variety of cell types, such as stem cells and cancer cells, were exposed to 3D environments [20–24]. Cells were grown to form spherical aggregates, which were different from those grown on planar surfaces. We believe that the aggregation of cells could be attributed to the cell–matrix and cell–cell interactions. Furthermore, certain signaling pathways of cells could be influenced by modifying the properties of the hydrogel [24]. Based on our previous experience, we developed a 3D cell-culture platform based on a hydrogel for MIN6 cells, in which the physical properties such as elastic modulus, stress relaxation, and cell adhesion were modified. Cell morphology, viability, insulin content, glucose-stimulated insulin secretion, and the associated gene and protein expressions were determined and compared with that of the 2D cell-culture system. The aim of this study is to develop and characterize a novel 3D cell-culture platform that can improve long-term pancreatic islet β -cell viability and function, which can serve as a persistent glucose-responsive source of insulin and islet transplantation treatment in the near future.

2. Materials and methods

2.1. Materials

Millipore water ($18.25 \text{ M}\Omega \text{ cm}^{-1}$), prepared with a Milli-Q Plus water system, was used throughout the experiments. Poly(ethylene glycol) diacrylate (PEGDA 2000 Mw) was purchased from Sigma-Aldrich Inc. GelMA with 20% degree of substitution was purchased from Tissue Ink Co., Ltd. Lithium phenyl-2,4,6-trimethylbenzoylphosphinate (LAP) was purchased from StemEasy Inc.

Unless stated otherwise, all other reagents were purchased from Aladdin Industrial Inc.

2.2. Preparation of the GelMA/PEGDA composite hydrogel

Hydrogels with different mechanical properties were prepared by adjusting their formulas individually. The following example describes the preparation parameters and processes of hydrogels. For multicellular spheroid (MCS)-culturing hydrogels, PEGDA (10 mg), N, N'-methylene-bis-acrylamide (0.2% wt.), and GelMA (80 mg) were added to 1 mL of water and dissolved at 50°C for 2 h, while for monolayer cell (MLC)-culturing hydrogels, PEGDA (60 mg), N, N'-methylene-bis-acrylamide (0.2% wt.), and GelMA (120 mg) were added. Then, LAP (5 mg) was added to the above mixture respectively and dissolved for 5 min. Then, the above mentioned precured gel solution was injected into a customized cylindrical mold (diameter: 3 cm; thickness: 1 mm) and irradiated under 405 nm visible light for 10 s to polymerize the GelMA/PEGDA hydrogel. The composite hydrogels were dipped and rinsed with millipore quality water every 8 h for 3 days. After sterilization with ethylene oxide, the hydrogels were ready for use in cell culture.

2.3. Stiffness measurement of composite hydrogel

The Young's modulus of the hydrogel was characterized by the Piuma Nanoindenter (Optics11, The Piuma, Netherlands). The prepared hydrogel was placed on the working table of the Piuma Nanoindenter, and its mechanical properties were collected at different positions by using the Optics11 PIUMA probe of the nanoindenter and dedicated Piuma software.

2.4. Cell culture conditions

The mouse pancreatic β -cell line MIN6 was grown and cultured in DMEM (Sigma-Aldrich, St. Louis, MO) supplemented with 15% FBS (Gibco, Burlington, Ontario, Canada), 100 $\mu\text{g}/\text{mL}$ streptomycin, 100 units/mL penicillin, 10 mmol/L HEPES, and 50 $\mu\text{mol}/\text{L}$ β -mercaptoethanol (Sigma-Aldrich, St. Louis, MO). All cell cultures were incubated at 37°C in humidified 95% air–5% CO_2 atmosphere. MIN6 cells were seeded at a density of $0.2 \times 10^6/\text{well}$ on hydrogels in a six-well culture plate, and cultured for 7 days. Meanwhile, the MIN6 cells were seeded at a density of $0.2 \times 10^6/\text{well}$ in a six-well culture plate for comparison. To collect the cells for further studies, the cells were trypsinized via incubation with 0.25% (v/v) trypsin for 2 min at 37°C , followed by dilution in fresh DMEM. Then, the cell suspensions were centrifuged and washed twice with PBS.

2.5. Confocal live/dead cell imaging

The cell viability was assessed using the LIVE/DEAD™ Cell Imaging Kit (488/570) (Invitrogen) according to the manufacturer's protocol. The MIN6 cells were cultured under different conditions for 7 days and incubated with working reagents for 30 min at 25°C . Fluorescence images were analyzed using a confocal laser scanning microscope (Zeiss, LSM710).

2.6. Immunofluorescence staining

MIN6 cells cultured on different matrixes were fixed using 4% paraformaldehyde for 15 min at 4°C , permeabilized, and blocked with 0.3% NP-40/3% BSA in PBS for 30 min at room temperature. The primary antibodies used were rabbit anti-Laminin (1:200, Abcam), rabbit anti-Fibronectin (1:200, Abcam), mouse anti-E-cadherin (1:100, Cell Signaling Technology), mouse anti-N-cadherin (1:150, Cell Signaling Technology), and the secondary antibodies were Alexa Fluor®488 and Alexa Fluor®594 (1:200, Invitrogen). The nuclei were stained with DAPI (Sigma-Aldrich). After standard procedures for immunostaining, the

hydrogel was transferred to a confocal dish and confocal images were acquired using a confocal laser scanning microscope (Zeiss, LSM710).

2.7. Time-lapse microscopy

Time-lapse images of cells seeded either on cell culture plates or hydrogels were acquired every 15 min at 20 × magnification for 48 h, using an X-living cell workstation (Olympus).

2.8. Insulin secretion and content

Insulin secretion measurements were performed using glucose-stimulated insulin secretion (GSIS). The cells were seeded in 12-well plates. The cells were washed and then incubated in HEPES-balanced Krebs-Ringer bicarbonate buffer (KRBH) (115 mmol/L NaCl + 4.7 mmol/L KCl + 1.2 mmol/L MgSO₄ · 7 H₂O + 1.2 mmol/L KH₂PO₄ + 20 mmol/L NaHCO₃ + 16 mmol/L HEPES + 2.56 mmol/L CaCl₂ + 0.2% BSA) for 0.5 h. After incubation, for the GSIS assay, the MIN6 cells were incubated for 1 h in KRBH with low glucose (containing 2 mmol/L glucose) or stimulatory glucose (containing 20 mmol/L glucose). Insulin was measured in the supernatant collected after the incubation. The supernatants were stored at −80 °C prior to insulin analysis by an enzyme-linked immunosorbent assay (ELISA) using a mouse insulin immunoassay kit (EZassay, MS200), according to the manufacturer's protocol. The glucose stimulation index (GSI) was calculated by dividing the insulin secretion at 20 mM by the insulin secretion at 2 mM glucose.

The cells cultured under different conditions were collected and lysed for protein quantification using a bicinchoninic acid (BCA) assay. The results of the insulin ELISA were normalized to the amount of protein from the corresponding cells. The BCA assay was performed on the cell suspension post-lysis, according to the manufacturer's instructions (ThermoFisher Scientific).

2.9. Quantitative real-time PCR analysis of GAPDH, Pdx1, NeuroD1, Piezo1, and Rac1

The total RNA was isolated from the MIN6 cells under different conditions using RNAiso Plus (Takara) following the manufacturer's protocol. Reverse transcription reactions were performed using 1 µg of total RNA and PrimeScript™ RT reagent kit (Takara). Quantitative real-time PCR (qPCR) was performed using SYBR® Premix Ex Taq (Takara) with the specific primers listed in Table 1. The relative expression was calculated using the 2^{−ΔΔCt} method normalized by GAPDH. Each experiment was repeated at least three times and each sample was analyzed in triplicate.

2.10. Western blot analysis

MIN6 cells harvested from the hydrogel were lysed in RIPA buffer (50 mmol/L Tris-HCl pH8.0, 150 mmol/L NaCl, 1% TritonX-100, 100 µg/mL PMSF, and protease inhibitor cocktail) on ice for 30 min. The lysate was clarified by centrifugation for 20 min at 12000 rpm at 4 °C. The protein concentration was determined using the BCA assay, and equal amounts of protein (30 µg) were loaded onto a 10% SDS-PAGE gel. After electrophoresis, the proteins were transferred to a PDVF membrane (Millipore). The membrane was blocked in 5% nonfat milk for 1 h

and then incubated with a primary antibody overnight at 4 °C. A horseradish peroxidase (HRP)-labeled secondary antibody was added against the primary antibody for 2 h at room temperature. The blots were visualized using an enhanced chemiluminescence detection system. The primary antibodies used were anti-β-actin (Zenbio, 200068-8F10), anti-GAPDH (Zenbio, 200306-7E4), anti-Pdx1 (Proteintech, 20989-1-AP), anti-NeuroD1 (Proteintech, 12081-1-AP), anti-Piezo1 (Proteintech, 15939-1-AP), and anti-Rac1 (Proteintech, 24072-1-AP).

2.11. Statistical analysis

At least three independent experiments were performed. Comparisons were performed using the Student's t-test between two groups or 2-way ANOVA in multiple groups. The results were presented as the mean ± SD. P < 0.05 was considered statistically significant.

3. Results

3.1. 3D cell-culture system based on hydrogels with tunable material microenvironment properties

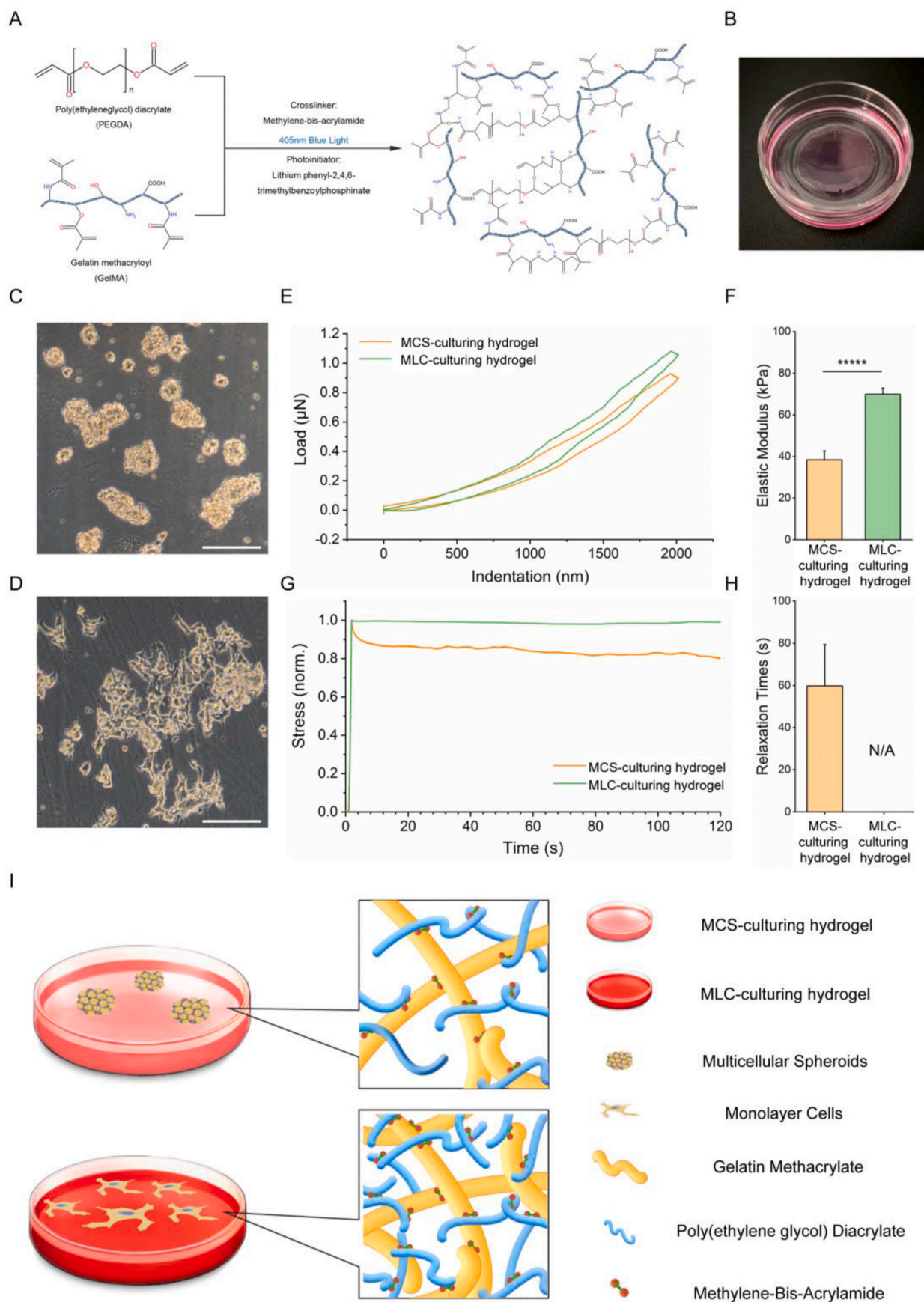
The (bio)physical properties of the hydrogel platform is tunable, through adjusting the mass ratio between GelMA and PEGDA and the overall mass percentage of these two components, supported by Young's modulus and stress relaxation data. It was hypothesized that such changes could provide MIN6 cells with distinctive mechanical and adhesion microenvironments, ultimately resulting in cells residing in these niches behaving differently. This hypothesis was validated on mouse embryonic fibroblasts (MEFs) based on our previous observation [24]. The chemical structures and photograph of the hydrogel are presented in details in Fig. 1A and B. In the present study, we showed two representative conditions, in which conditions MIN6 cells could typically form multicellular spheroids (Fig. 1C) or monolayers (Fig. 1D), after 7 days of culturing the cells on the surface of these hydrogels. Based on this finding, we named the low-GelMA-ratio hydrogels as multicellular spheroid (MCS)-culturing hydrogels and the high-GelMA-ratio ones as monolayer cell (MLC)-culturing hydrogels (Fig. 1E). The specifications are as follows: corresponding to MCS-culturing hydrogel or MLC-culturing hydrogel, the mass ratio, in the form of GelMA: PEGDA (mass to mass), was 8:1 or 2:1, and the overall mass percentage, in the form of (GelMA + PEGDA)/water × 100%, was 9% or 18%, respectively. This finding inspired us to further explore the major microenvironmental factors that drove such behavioral changes in MIN6 cells. The Young's modulus and stress relaxation of these two types of hydrogels were measured by the nanoindenter; with the stress-strain curves of these two materials and the calculated Young's modulus are shown in Fig. 1E and F, respectively. Fig. 1G–H shows the stress-time curve and the calculated stress half-relaxation time (t_{1/2}) measured with the same experimental settings. The Young's modulus of the MLC-culturing hydrogel was found to be significantly higher than that of the MSC-culturing hydrogel; nevertheless, both of them had the same order of magnitude (69.95 ± 2.89 kPa vs. 38.38 ± 4.25 kPa). However, the MLC-culturing hydrogel displayed almost time-independent stress curve and negligible stress relaxation. In contrast, the MSC-culturing hydrogel exhibited time-dependent stress curve with half the stress-relaxation time (t_{1/2}) in 59.80 ± 19.62 s. This set of data manifested the distinctions (elastic vs. viscoelastic) of the mechanical behaviors between these two types of hydrogels, and we speculated that this stress relaxation distinction dominantly drove the different MIN6 cell behaviors cultured on these two types of materials.

3.2. Morphology and viability of MIN6 cells cultured on composite hydrogel as a 3D cell culture matrix

MIN6 cells were cultured on hydrogels with different parameters, as well as on polystyrene cell-culture plates. After 7 days of culture

Table 1
Primers used for qPCR.

Gene	Forward primer	Reverse primer
GAPDH	CCAGTATGACTCCACTCACG	GACTCCACGACATACTCAGC
Pdx1	GATGTTGAACCTTGACCGAGAGA	GTCCCGCTACTACGTTTCTTATC
NeuroD1	CACGAGGCAGACAAGAAAGA	TCCTCTTCCTCTAGATCCTCATC
Piezo1	GCCGAGAGACAGAGAAGAAATAC	GGCGATGAGGAAGAGATAATG
Rac1	TGTCCGTGCAAGTGGTATC	AGCTTCTCAATGGTGTCTTATC



(caption on next page)

Fig. 1. Hydrogel with tunable microenvironment properties as multicellular spheroid (MCS) and monolayer cell (MLC)-culturing substrate. Schematic of the chemical structure of PEGDA and GelMA. Upon mixing the PEGDA and GelMA with MBAA and LAP, a hydrogel network is formed via photoinitiation (405 nm blue light) (A). Photograph of hydrogel as cell-culturing substrate (B). Optical microscope images of MIN6 cells cultured on hydrogels with different microenvironment properties. By tuning the physical properties of the hydrogels, the state of aggregation of MIN6 cells varied from multicellular spheroids to clustered monolayer (C, D). Scale bar: 200 μ m. Elasticity tests (E, F) and stress relaxation tests (G, H) of MCS-culturing hydrogel and MLC-culturing hydrogel. Schematic of MIN6 cells cultured on hydrogels with different microenvironment properties (I). The data is represented as means \pm standard deviation. An n of 6 was used and analyzed using a one-way ANOVA with multiple comparisons. **** $p < 0.00001$. (For interpretation of the references to colour in this figure legend, the reader is referred to the Web version of this article.)

(Supplemental Fig. 2), the control cells on the cell-culture plate grew as a monolayer; they were partially spread and formed small aggregates. Cells seeded on MLC-culturing hydrogels grew as a tightly clustered monolayer, and the clusters were similar in morphology but larger in

size when compared to those grown on commercial culture plates. Cells exhibited multicellular spheroids after growth on MCS-culturing hydrogels, which were analogous to round pancreatic islet-like aggregates of cells adhering to the surfaces of the hydrogels. Images of live/

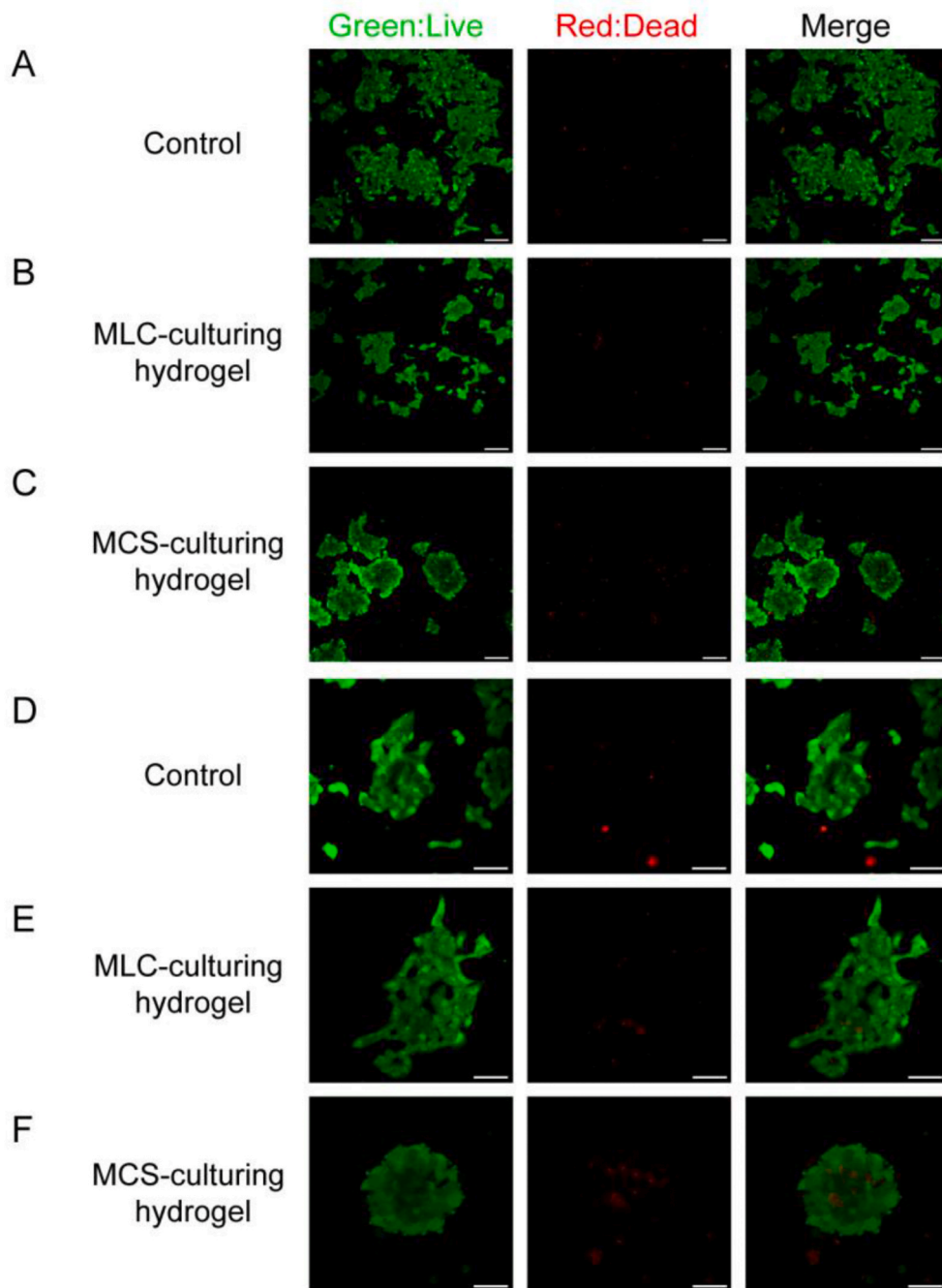


Fig. 2. MIN6 cells were cultured and grown on 2D cell-culture plates (A, D) and MLC (B, E) and MCS (C, F)-culturing hydrogels for 7 days, at 10 \times (A–C) and 20 \times (D–F) magnification, respectively. Representative scan of live/dead staining, green and red labeled cells denote living and dead cells, respectively. Scale bar: 10 \times : 100 μ m and 20 \times : 50 μ m. (For interpretation of the references to colour in this figure legend, the reader is referred to the Web version of this article.)

dead staining of cells obtained by laser scanning confocal fluorescence microscopy demonstrated that almost all the cells in spreading or aggregated forms were alive under different culture conditions (Fig. 2), which indicated the maintenance of quite high viability.

Moreover, to observe the formation process of monolayers or multicellular spheroids on the surfaces of different matrixes, the time-lapse images of the seeded cells were acquired every 15 min at 20 × magnification for 48 h using an Olympus X-living cell workstation (Supplementary video materials). Fig. 3A–C shows that the MIN6 cells were split and spread as a monolayer in the 2D culture system on planar plate, while in the 3D culture system (Fig. 3D–F and 3G–I), the cells initially formed small aggregates, which further merged into irregular clusters or spheroids.

Supplementary video related to this article can be found at <https://doi.org/10.1016/j.biomaterials.2021.120687>.

3.3. Fibronectin (FN), laminin (LN), N- and E-cadherin (N-cad and E-cad) expressions in MIN6 cells by immunofluorescence staining

To obtain information and clues on the cell–matrix and cell–cell interactions in 2D and 3D cell-culture systems, the distributions of adhesion proteins including FN and LN, N-cad, and E-cad were studied by fluorescent cytochemistry and confocal laser scanning microscopy. As shown in Fig. 4, the “Control” group (Fig. 4A and D) exhibits the 2D cell-culture system in which the cells were cultured on planar cell-culture plate. Meanwhile, the 3D cell-culture systems include both experimental groups of “MLC-culturing hydrogel” (Fig. 4B and E) and “MCS-culturing hydrogel” (Fig. 4C and F), indicating the cells were grown in the 3D culturing systems based on hydrogels. FN and LN are the major ECM proteins of islets. The results shown in Fig. 4A–C demonstrate that FN was not or only a little detectable in the control cells on the cell-culture plate or MLC-culturing hydrogel, whereas, the cells grown on

the MCS-culturing hydrogel exhibited greatly enhanced fluorescent signals. The obvious increase in the level of the FN signal in multicellular spheroids could indicate improved functioning of the MIN6 cells and more native environments of islets, when compared to that under 2D culture conditions. N-cad and E-cad were observed under all conditions (Fig. 4A–F), since cadherins are involved in the maintenance of β -cell viability. Ca^{2+} -dependent homophilic cell adhesion between β -cells within islets was mediated by E-cad, and its function was implicated as a mechanism for cell migration and cell growth, particularly, for regulating β -cell proliferation in islet-like structures [25].

3.4. Insulin secretion and content measurements

For insulin secretion studies, GSIS was performed using low and high concentrations of glucose to stimulate the phases of insulin secretion. MIN6 cells were grown on cell-culture plates and hydrogels for 7 days, and insulin secretion was determined after 2 h static incubation at 2 or 20 mM glucose. The MIN6 cells readily secreted insulin, and the clusters and spheroids were more efficient at secreting insulin in response to glucose with larger amounts of released insulin (Fig. 5A). On MCS-culturing hydrogels, the cells showed significant increase in glucose-induced insulin secretion at 20 mM than at 2 mM glucose. The glucose stimulation indexes (GSI; ratio between insulin secretion at 20 mM and at 2 mM glucose) were slightly higher in the case of hydrogel conditions (Table 2); however, the values were not significantly different among the different conditions. The insulin content of the MIN6 cells was sensitive to the substrate, and an increase of approximately 7.3–7.9 folds was observed in the cellular insulin content (relative to the amount of protein) for the MCS and MLC-culturing hydrogels, when compared to the control cells (Fig. 5B).

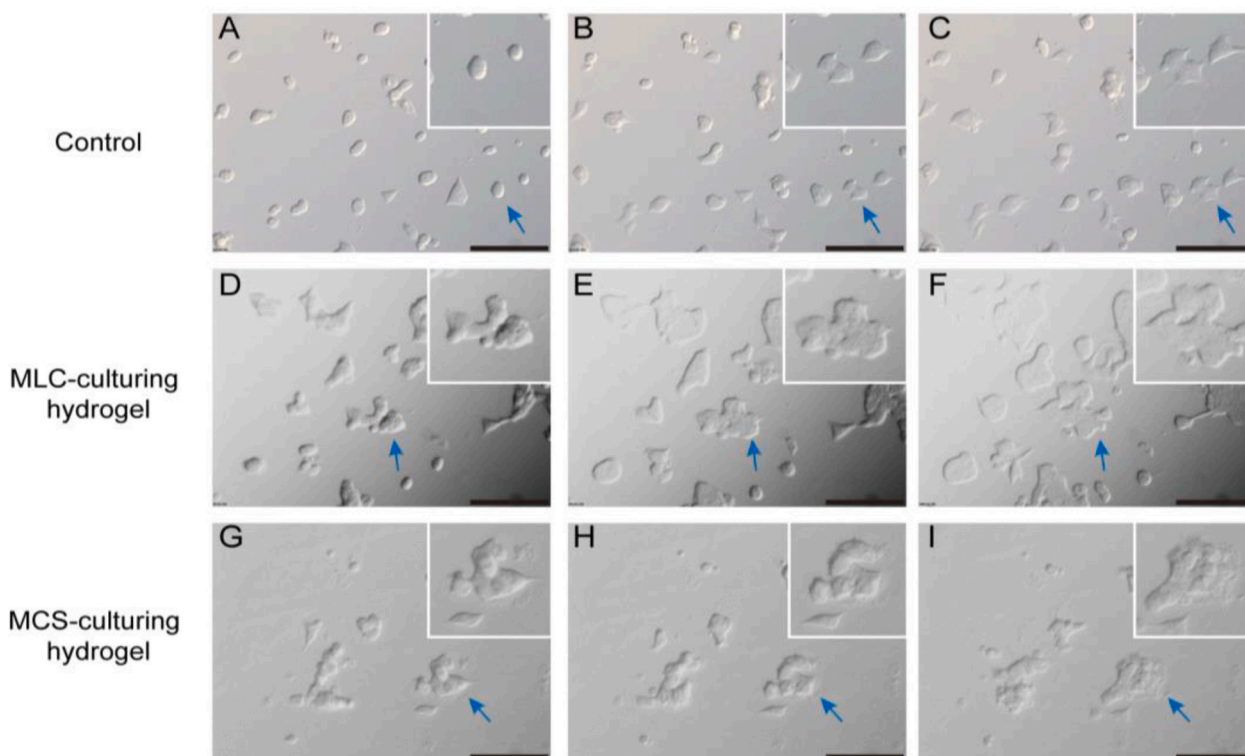


Fig. 3. Time-lapse microscope images of MIN6 cells cultured on cell-culture plate (A–C), MLC (D–F) and MCS (G–I)-culturing hydrogels after cell seeding for a duration of 48 h. Blue arrows point to the spontaneous formation process of monolayer on culture plate or clustered monolayers and multicellular spheroids on hydrogels via migration, proliferation, and mergence. Scale bar: 100 μm . (For interpretation of the references to colour in this figure legend, the reader is referred to the Web version of this article.)

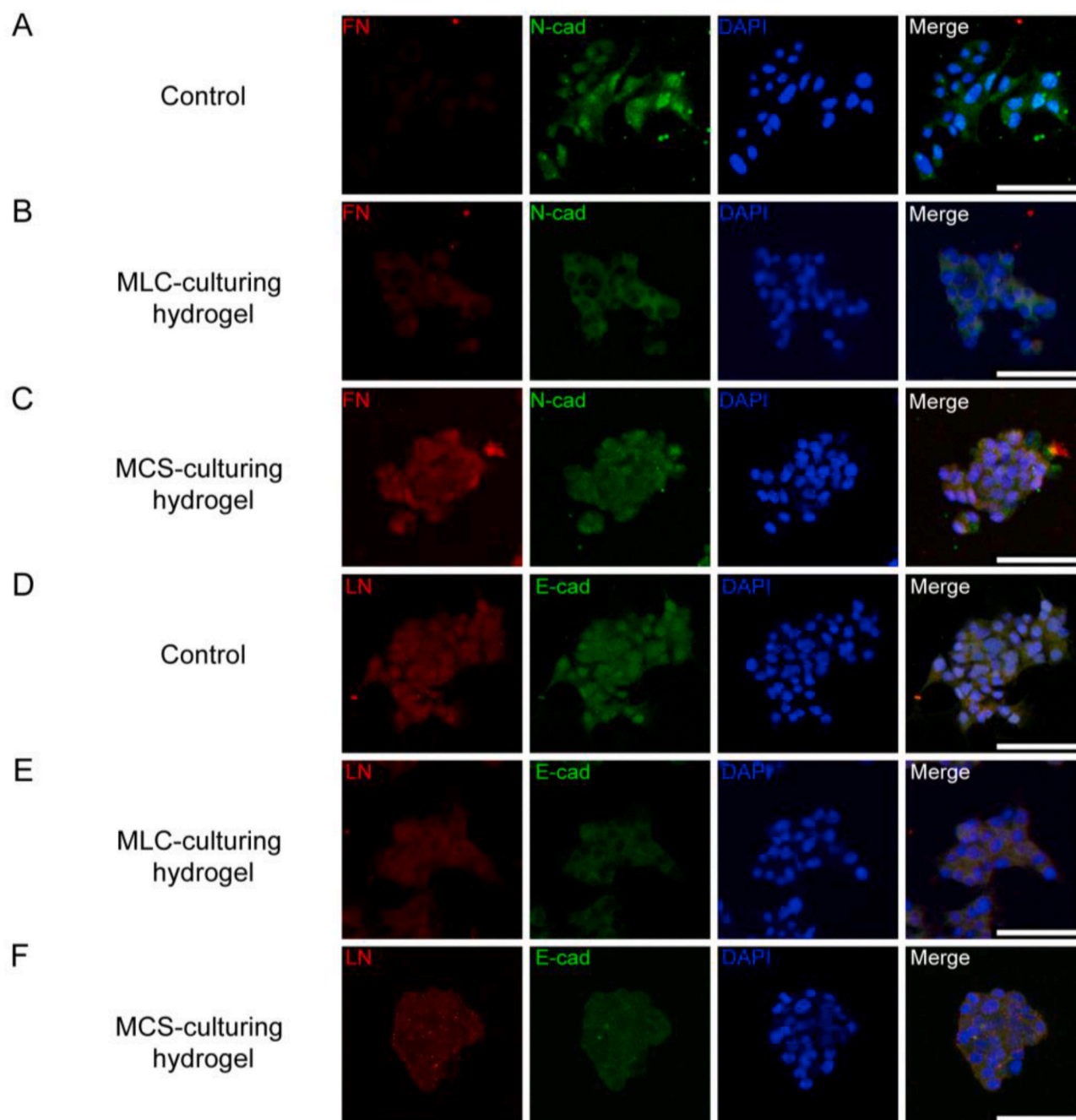


Fig. 4. Immunofluorescence staining of fibronectin (FN, red staining) and N-cadherin (N-cad, green staining) (A, B, C), laminin (LN, red staining) and E-cadherin (E-cad, green staining) (D, E, F) in control group (A, D), monolayer clusters (B, E) and multicellular spheroids (C, F); blue staining represents DAPI-positive nuclei. Images were taken at 40 × magnification. Scale bar: 50 μm. (For interpretation of the references to colour in this figure legend, the reader is referred to the Web version of this article.)

3.5. Gene and protein expression of β -cell transcription factors

To examine the effects of different culture conditions on the β -cell function, gene expression of the critical transcription factors of insulin, including pancreatic and duodenal homeobox1 (Pdx1) and neuronal differentiation 1 (NeuroD1) were analyzed. These two transcription factors play key roles in the maturation, identity, and regeneration of β -cells. They also interact with each other to activate the transcription of the insulin promoter in β -cells [26,27]. Pdx1 regulates β -cell functions such as insulin expression to a great extent. Inactivation of NeuroD has been reported to be responsible for the loss of islet cells in mice, particularly, in β -cells, because of apoptosis [28], which is a strong

inductor of insulin. As shown in Fig. 6, hydrogels facilitate tightly clustered monolayer and multicellular spheroid formation can improve insulin processing. Hydrogels increased Pdx1 and NeuroD1 expression significantly above the control levels (Fig. 6A–B). The MCS-culturing hydrogel showed 11.5 fold increase in Pdx1 and 2.6 fold increase in NeuroD1, compared to the control group. A significant 3.7 fold increase in Pdx1 and 1.5 fold increase in NeuroD1 between the MCS and MLC-culturing hydrogel groups were observed. Furthermore, as shown in Fig. 6E–F, significant enhancement of Pdx1 and NeuroD1 protein expression in cells grown on hydrogels was confirmed by Western blot analysis, and this trend was similar to the mRNA expression. The hydrogel-constructed 3D system promoted significantly higher levels of

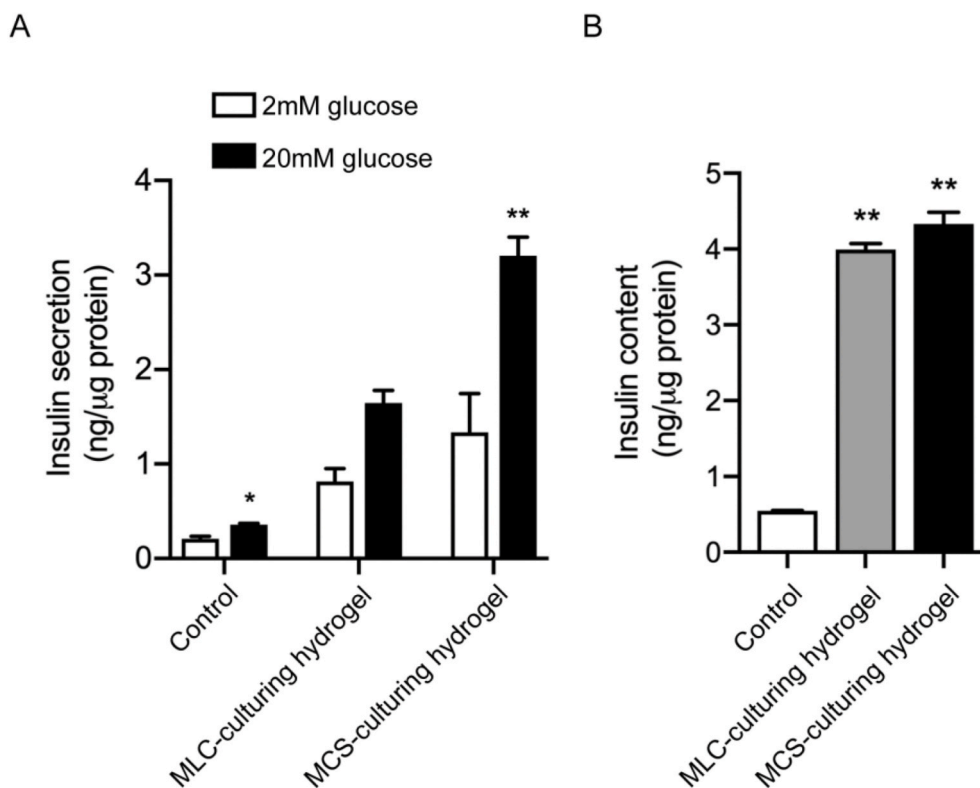


Fig. 5. MIN6 cells were cultured on 2D cell-culture plates (control) and MLC and MCS-culturing hydrogels, and after growing for 7 days, insulin secretion (blank bars: 2 mM glucose, black bars: 20 mM glucose) (A) and insulin content (B) normalized to the amount of protein from the corresponding groups measured by GSIS and Elisa assays. Values are mean \pm SD, $n = 3-6$. * $P < 0.05$, ** $P < 0.01$.

Table 2

Glucose stimulated index (GSI; ratio between insulin secretion at 20 mM and at 2 mM glucose) normalized to the amount of protein from MIN6 cells measured by GSIS and Elisa assay. Values are mean \pm SD, $n = 3-6$.

	Control	MLC-culturing hydrogel	MCS-culturing hydrogel
Glucose stimulation index (GSI)	1.72 \pm 0.05	2.02 \pm 0.09	2.40 \pm 0.05

expression of these transcription factors, where MCSs and MLCs significantly presented 2.3 and 1.6 fold increases, respectively, in Pdx1; and 3.0 and 2.0 fold increases, respectively, in NeuroD1, when compared to the control condition. The rising trend between the two types of hydrogel groups (MCS vs. MLC) was significant as well.

Recently, it was found that Piezo ion channels were responsible for the mechanical responses in cells. A mechanically activated Ca^{2+} -permeable cationic channel, called “Piezo1” was identified in various types of mammalian cells [29,30]. It is known that the insulin release process is induced by cell swelling, which might be affected by the stimulation of the Ca^{2+} -permeable stretch-activated channels on the cell membrane; therefore, Piezo1 mRNA and protein levels were detected in this study. As shown in Fig. 6C and E–F, the relative mRNA and protein-expression levels of Piezo1 were significantly higher in the 3D culturing system of hydrogels than in the 2D culture plate (control group). 1.9 and 1.3 fold increases in mRNA and protein amounts were measured between the MCSs and MLCs, respectively. These results indicated that the MIN6 cells were mechanosensitive to the cellular microenvironments and that the insulin secretion of the cells was related to the activation of Ca^{2+} -permeable cationic channels.

Ras-related C3 botulinum toxin substrate 1 (Rac1) is a member of the Rho family of small GTP-binding proteins, which has been identified in β cells, and was reported to be involved in regulating the morphogenesis

of pancreatic islets, playing a vital role in cell migration and cell adhesion [31]. In addition, Rac1 was found to regulate glucose-stimulated insulin secretion [32,33], and the knockdown of Rac1 was found to result in the inhibition of insulin secretion. As shown in Fig. 6D and E–F, MCS and MLC-culturing hydrogel groups presented 1.6 and 1.3 fold increases in Rac1 mRNA expression, and 2.4 and 1.5 fold increases in Rac1 protein expression, respectively, when compared to the control cells. This indicated that the various morphologies of MIN6 cells grown in 2D and 3D culture systems could be attributed to the cytoskeleton deformations caused by cell migration and adhesion.

4. Discussion

In this study, by designing and modifying the physical properties of hydrogels, we developed a novel 3D cell-culture platform for MIN6 cells. We and others had previously identified that adhesion ligand density was one of the key regulators of spheroid formation [20,23], and it was reported that the adhesion ligand density of this platform was dependent on the GelMA ratio [24]. However, when considering the physicochemical properties of GelMA and PEGDA, which comprised the hydrogel network, we proposed that the mechanical properties of the matrixes could also vary depending on the mass ratio between GelMA and PEGDA. Our data with respect to Young’s modulus and stress relaxation of MCS and MLC-culturing hydrogels confirmed this point. Although it was not demonstrated in the present study, that the delineation of Young’s modulus or stress relaxation of this hydrogel platform under different conditions in terms of mass ratio or overall mass percentage, we previously showed the feasibility of such method in tuning the Young’s modulus of a similar hydrogel platform (GelMA + polyacrylamide) by adjusting the mass ratio of GelMA then profiling the Young’s modulus of the hydrogel platform [24]. In particular, we found that the MSC-culturing hydrogel was viscoelastic, while the MLC one was elastic. This is important because, unlike the properties of elastic

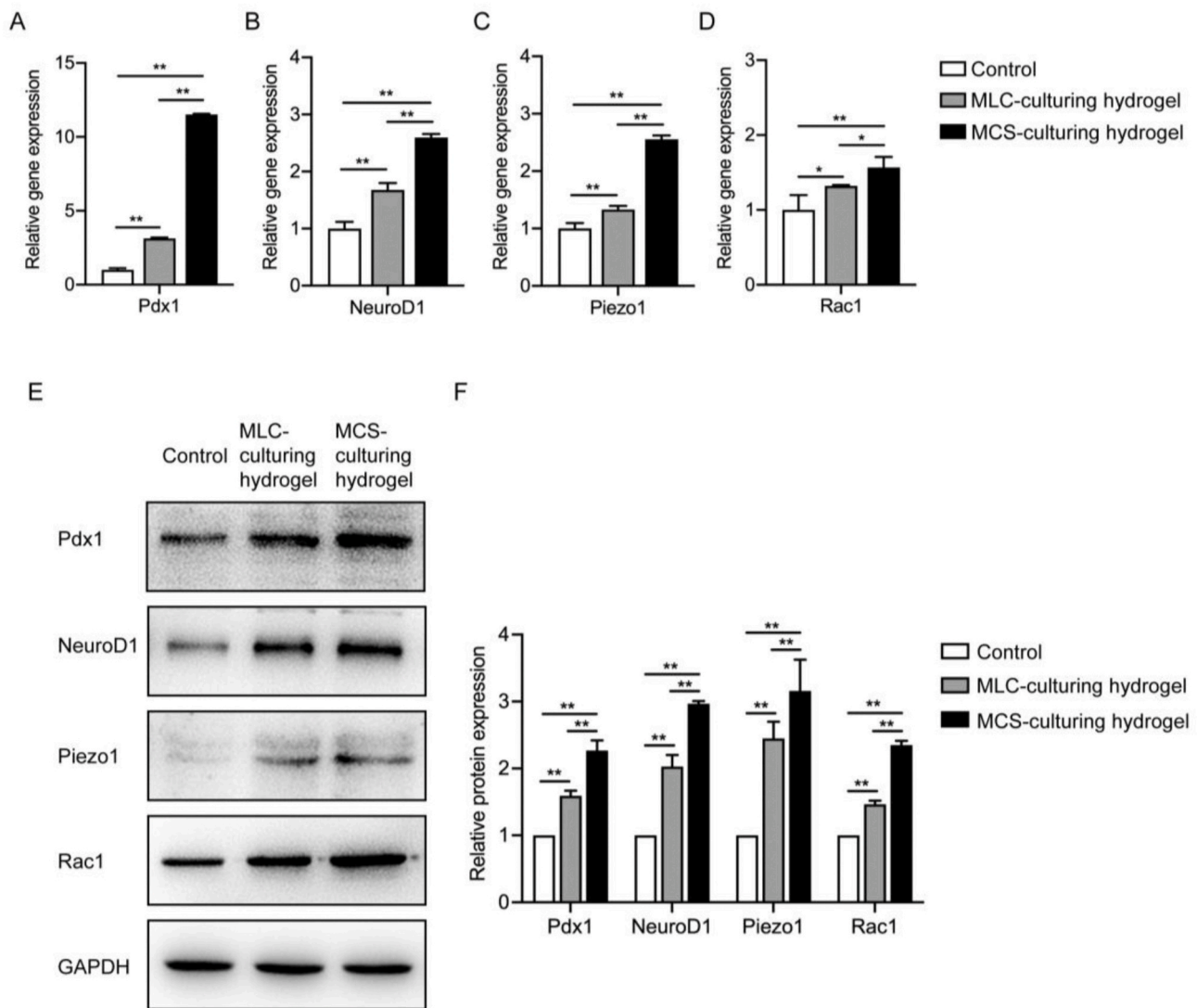


Fig. 6. Gene expression (A–D) and Western blot analysis (E, F) of the transcription factors Pdx1, NeuroD1, Piezo1, and Rac1 in MIN6 cells cultured on cell-culture plate (blank bars: control group) and hydrogels (grey bars: MLC-culturing hydrogel and black bars: MCS-culturing hydrogel) after 7 days. The relative gene and protein expression were calculated after normalization to the GAPDH. Values are mean \pm SD, $n = 4-6$. * $P < 0.05$, ** $P < 0.01$ vs. Control.

materials, the mechanical properties of viscoelastic materials are time-dependent, which provides cells with a highly dynamic mechanical microenvironment in the extracellular niches. This could sequentially regulate the sensing and interperception of mechanical input by cells through different levels in mechanotransduction cascades (e.g., surface adhesion receptors, cytoskeletons, transcriptional programs, etc.), and ultimately influence the outputs of the cells, which are manifested through different cell behaviors such as cell spreading, stem-cell fate [19,34], and MCS formation. We therefore speculated that the presence of viscoelasticity in MCS-culturing hydrogels, which was absent in the MLC-culturing hydrogels, was another key factor that determined the formation of MCSs. It is worth noting here that various living tissues (e.g., adipose, liver, brain, etc.) and ECM materials (e.g., collagen, fibrin, etc.) are viscoelastic and exhibit stress relaxation as well [29]. This type of dynamic, time-dependent mechanical interplay is universally presented between cells and microenvironmental niches in real tissue/organs.

It was found that the morphology of MIN6 cells varied from monolayers and clusters to multicellular spheroids on different surfaces, which was in accordance with a previous report that stated that primary β cells were mechanosensitive in response to tissue stiffness [10]. It has been observed elsewhere that MIN6 cells tend to assemble to form

pseudo-islets where more cell–cell interactions are required [35,36]. In addition, similar results were demonstrated in other β -cell lines [10,37], as well as in different cell types such as tumor cells [21–23] and stem cells [11], when applying hydrogel as a 3D cell-culture scaffold. The formation of cell aggregates or multicellular spheroids could be due to the surrounding ECM with insufficient cell–matrix adhesion function, such as scaffolds constructed by electrospinning or stimuli-responsive hydrogels, which forced cells to contact each other and then increased the cell–cell interactions [38,39]. Moreover, the fate of the cells was not decided by only one factor, rather, a combination of various physical properties was involved.

According to the morphological images, primary immunofluorescence staining studies were performed to observe cell–matrix and cell–cell interactions under 2D and 3D cell-culture conditions. FN and LN were shown to contribute to β -cell differentiation and islet development [40,41]. In addition, it was reported that they could induce the expression of islet cell markers [29], and enhance insulin secretion and glucose responsiveness [42]. Both N-cad and E-cad were observed and were found distributed within the cells, which was in accordance with the previous findings that pancreatic islet cell–cell adhesion was cadherin-mediated [43,44]. N-cad was found to express preferentially in β cells and to protect the cells from apoptosis [45]. However, the

different levels observed by immunofluorescence could also be due to the variable affinity or specificity of antibodies. Further studies of proteins and associated signaling pathways involved in cell–matrix and cell–cell interactions should be considered.

It has been shown in this study that the formation of clustered monolayers and spheroids in a 3D culture system greatly enhances insulin synthesis and secretion, while cell survival is high. Similarly, the so-called “pseudo-islets” form shows superior function of insulin release than isolated cells [46,47]. The reason why the overall insulin secretion is significantly lower in the control group might be attributed to the following aspects: firstly, it is well known that rodent islets behave differently in Petri dishes or in vitro perfusion systems, according to the knowledge about how islets behave in their native environment in the pancreas. The islet cells tend to form aggregates in their nature behavior. Therefore, the control group, which stands for the 2D cell-culture system where MIN6 cells were grown on the planar surface of cell culture plate, actually provided the cells with an unfavorable microenvironment that substantially distinctive from the native ones, and potentially compromise the secretion capabilities of the cells, compared to the hydrogel platforms. Secondly, nutrients and the cell metabolism can markedly affect glucose-stimulated insulin secretion. Given that β -cells are continually exposed to a complex milieu of nutrients, they continuously couple nutrient metabolism to modulate the synthesis and release of insulin. Both the MLC and MCS-culturing hydrogels were fully immersed in culture media for hours before use, therefore can deliver nutrients, so that the cells could get more nutrients from the hydrogel matrix compared to the plastic surface of the Petri dish. Thirdly, the insulin synthesis in experimental groups is remarkably higher than the control group, which spontaneously results in a higher amount of insulin secretion. The promotion of cell function could be explained by cell–matrix interactions, biochemical signaling interactions, and an increase in glucokinase enzyme activity [27,40,48]. This great enhancement was also reported between β cells embedded in islets and isolated β cells [49,50]. Moreover, it was found that baseline secretion was also strongly increased on the hydrogels, so that the changes in the values of GSI were not significantly different, although an increase in insulin expression on substrates of hydrogels was observed. The changes in the surrounding microenvironments from 2D to 3D could be the reason for the variation in baseline secretion, which should be studied further.

To explore the underlying mechanisms, the mRNA expression of typical insulin-transactivating factors including Pdx1 and NeuroD1 were analyzed. The inactivation of Pdx1 in β cells in mice was found to cause diabetes [51,52]. The relative fold increase in Pdx1, expressed in MIN6 cells on hydrogels when compared with that on the culture plate in this study, was of the same magnitude as that in other studies [53]. The trend of NeuroD1 expression in 2D and 3D culture systems found here had also been observed elsewhere [54]. In this study, a significant increase in Piezo1 mRNA and protein expression levels were measured on hydrogels, and Piezo1 agonists were suggested to be used as enhancers of insulin release from INS-1 cells (one of rat β -cell lines), as the Piezo1 channel agonist was reported to be involved in cell-swelling-induced insulin release [30]. In further studies, patch clamp experiments can be designed to measure insulin transportation and the corresponding changes in Ca^{2+} -permeable cationic channels through cell membranes. Some groups have reported that Rac1 participates in insulin secretion in the pancreatic β -cell line via the modulation of cytoskeleton and cell–cell contact, where the inhibition of Rac1 functions cause decreased insulin secretion [31,32,55,56]. Moreover, the improper movement of Rac1 results in glucotoxicity [57]. Therefore, a significant increase in Rac1 mRNA and protein expression levels on hydrogels, found in this study, might contribute to the formation and genesis of MLCs and MCSs as well as increased insulin secretion.

Various methods have been developed for insulin-secreting cells or tissues that maintain proper cellular function and stable glucose-induced insulin secretion, such as modifying the composition of specific cell-culture media, adding growth factors that stimulate insulin

production, coculture together with other cell types, and so on [58,59]. This study implies that, in addition to the previous strategies, 3D cellular microenvironments are of great importance as well. Fig. 7 presents a general hypothesis of the current and further studies drawn by us. It demonstrates that insulin expression is increased not only by cluster formation but also in response to a combination of the stiffness, stress relaxation, and adhesion ligands of the corresponding cellular microenvironments. In this highly dynamic 3D microenvironment provided by the fabricated viscoelastic materials, the cell behavior and insulin synthesis and secreting function of MIN6 cells are influenced by a combination of various factors including cell–ECM and cell–cell interactions with related proteins such as integrin, cadherin, and catenin, ion channels on the cell membrane, cytoskeleton deformation modulated by Rac1/ROCK/MLCK pathway [54], and insulin transcription factors such as Pdx1, NeuroD1, MafA, and SCD1.

5. Conclusion

In conclusion, we proposed a novel 3D cell-culture system that was based on a hydrogel for MIN6 cells, which can be a previously under-acknowledged regulator that guides the pancreatic β -cell response. MIN6 cells could adhere to the substrate and form multicellular spheroids (MCSs) via self-organization. Compared to the conventional 2D cell-culture method based on planar plates, we found that the insulin synthesis and glucose sensitivity were significantly enhanced by tuning the

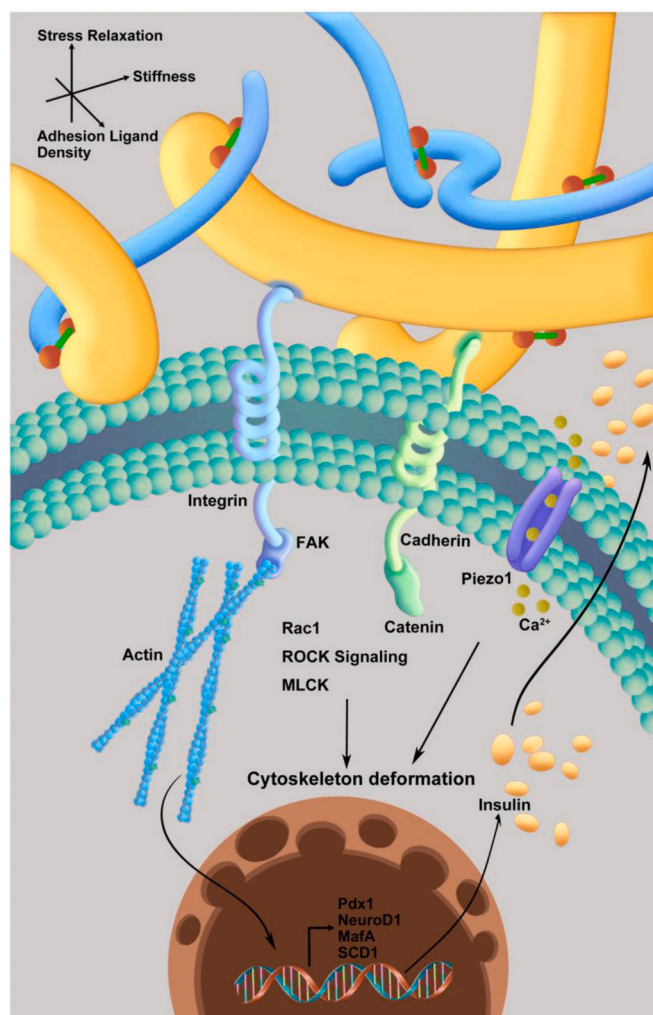


Fig. 7. Overview of how microenvironmental properties of hydrogels couple to improve the insulin-secreting function of MIN6 cell.

physical properties of the hydrogel matrices. This is the first study that investigates a combination of multiple physical properties of biomaterials on β -cell cluster insulin processing. We believe that this 3D cell-culture strategy will be a promising platform for diabetes treatment in clinical islet transplantation.

Credit author statement

Miao Zhang: Conceptualization, methodology, data curation, formal analysis, writing—original draft, and funding acquisition. Sen Yan: Data curation, formal analysis, investigation, and methodology. Xueqin Xu: Resources, investigation, and validation. Tingting Yu and Zhaobin Guo: Conceptualization, writing—reviewing, and editing. Ming Ma: Conceptualization. Yi Zhang: Resources. Zhuxiao Gu: Writing—reviewing and editing. Yiwei Feng, Chunyue Du, and Mengqi Wan: Resources and methodology. Ke Hu: Conceptualization, methodology, funding acquisition, and supervision. Xiao Han: Conceptualization, methodology, and supervision. Ning Gu: Conceptualization, funding acquisition, and supervision.

Declaration of competing interest

The authors declare that they have no known competing financial interests or personal relationships that could have appeared to influence the work reported in this paper.

Acknowledgements

The authors thank Shijia Tang and Bowen Wang from the Nanjing Medical University for their collaborations on studies involving 3D cell culturing, and Yinyi Zhao and Jie Wu for drawing the schematics.

Appendix A. Supplementary data

Supplementary data to this article can be found online at <https://doi.org/10.1016/j.biomaterials.2021.120687>.

Funding

This work was supported by the National Key Research and Development Program of China (2017YFA0104301), National Natural Science Foundation of China (61821002, 81701824, 51832001, 81830024), Youth Foundation of Jiangsu Scientific Committee (BK20180374), China Postdoctoral Science Foundation (2017M621787), and Talent Introduction Foundation of Nanjing Medical University (2017RC07).

References

- [1] C.J. Nolan, P. Damm, M. Prentki, Type 2 diabetes across generations: from pathophysiology to prevention and management, *Lancet* 378 (2011) 169–181.
- [2] M.A. Atkinson, G.S. Eisenbarth, A.W. Michels, Type 1 diabetes, *Lancet* 383 (2014) 69–82.
- [3] V. Plaisance, G. Waeber, R. Regazzi, A. Abderrahmani, Role of microRNAs in islet β -cell compensation and failure during diabetes, *J Diabetes Res* 2014 (2014) 618652.
- [4] A.M. Shapiro, M. Pokrywczynska, C. Ricordi, Clinical pancreatic islet transplantation, *Nat. Rev. Endocrinol.* 13 (2017) 268–277.
- [5] P. Fiorina, A.M. Shapiro, C. Ricordi, A. Secchi, The clinical impact of islet transplantation, *Am. J. Transplant.* 8 (2008) 1990–1997.
- [6] J.A. Giraldo, J.D. Weaver, C.L. Stabler, Enhancing clinical islet transplantation through tissue engineering strategies, *J Diabetes Sci Technol* 4 (2010) 1238–1247.
- [7] S.J. Park, S. Shin, O.J. Koo, J.H. Moon, G. Jang, C. Ahn, et al., Functional improvement of porcine neonatal pancreatic cell clusters via conformal encapsulation using an air-driven encapsulator, *Exp. Mol. Med.* 44 (2012) 20–25.
- [8] M. Phillip, T. Battelino, E. Atlas, O. Kordonouri, N. Bratina, S. Miller, et al., Nocturnal glucose control with an artificial pancreas at a diabetes camp, *N. Engl. J. Med.* 368 (2013) 824–833.
- [9] Y. Teramura, O.P. Oommen, J. Olerud, J. Hilborn, B. Nilsson, Microencapsulation of cells, including islets, within stable ultra-thin membranes of maleimide-

- conjugated PEG-lipid with multifunctional crosslinkers, *Biomaterials* 34 (2013) 2683–2693.
- [10] C.E. Nyitrai, M.G. Chavez, T.A. Desai, Compliant 3D microenvironment improves β -cell cluster insulin expression through mechanosensing and β -catenin signaling, *Tissue Eng.* 20 (2014) 1888–1895.
- [11] M. Darnell, A. O’Neil, A. Mao, L. Gu, L.L. Rubin, D.J. Mooney, Material microenvironmental properties couple to induce distinct transcriptional programs in mammalian stem cells, *Proc. Natl. Acad. Sci. U. S. A.* 115 (2018) E8368–e8377.
- [12] R.J. Pelham Jr., Y. Wang, Cell locomotion and focal adhesions are regulated by substrate flexibility, *Proc. Natl. Acad. Sci. U. S. A.* 94 (1997) 13661–13665.
- [13] K.A. Beningo, C.M. Lo, Y.L. Wang, Flexible polyacrylamide substrata for the analysis of mechanical interactions at cell-substratum adhesions, *Methods Cell Biol.* 69 (2002) 325–339.
- [14] E. Cukierman, R. Pankov, D.R. Stevens, K.M. Yamada, Taking cell-matrix adhesions to the third dimension, *Science* 294 (2001) 1708–1712.
- [15] W.L. Murphy, T.C. McDevitt, A.J. Engler, Materials as stem cell regulators, *Nat. Mater.* 13 (2014) 547–557.
- [16] S.P. Evanko, S. Potter-Perigo, P.L. Bollyky, G.T. Nepom, T.N. Wight, Hyaluronan and versican in the control of human T-lymphocyte adhesion and migration, *Matrix Biol.* 31 (2012) 90–100.
- [17] M.L. Gardel, I.C. Schneider, Y. Aratyn-Schaus, C.M. Waterman, Mechanical integration of actin and adhesion dynamics in cell migration, *Annu. Rev. Cell Dev. Biol.* 26 (2010) 315–333.
- [18] E. Sackmann, How actin/myosin crosstalks guide the adhesion, locomotion and polarization of cells, *Biochim. Biophys. Acta* 1853 (2015) 3132–3142.
- [19] O. Chaudhuri, L. Gu, D. Klumpers, M. Darnell, S.A. Bencherif, J.C. Weaver, et al., Hydrogels with tunable stress relaxation regulate stem cell fate and activity, *Nat. Mater.* 15 (2016) 326–334.
- [20] K. Hu, J. Sun, Z. Guo, P. Wang, Q. Chen, M. Ma, et al., A novel magnetic hydrogel with aligned magnetic colloidal assemblies showing controllable enhancement of magnetothermal effect in the presence of alternating magnetic field, *Adv. Mater.* 27 (2015) 2507–2514.
- [21] Z. Guo, K. Hu, J. Sun, T. Zhang, Q. Zhang, L. Song, et al., Fabrication of hydrogel with cell adhesive micropatterns for mimicking the oriented tumor-associated extracellular matrix, *ACS Appl. Mater. Interfaces* 6 (2014) 10963–10968.
- [22] S. Tang, K. Hu, J. Sun, Y. Li, Z. Guo, M. Liu, et al., High quality multicellular tumor spheroid induction platform based on anisotropic magnetic hydrogel, *ACS Appl. Mater. Interfaces* 9 (2017) 10446–10452.
- [23] K. Hu, N. Zhou, Y. Li, S. Ma, Z. Guo, M. Cao, et al., Sliced magnetic polyacrylamide hydrogel with cell-adhesive microarray interface: a novel multicellular spheroid culturing platform, *ACS Appl. Mater. Interfaces* 8 (2016) 15113–15119.
- [24] T. Yu, K. Hu, Q. Xu, X. Xu, C. Du, Y. Zhao, et al., An easy-to-fabricate hydrogel platform with tunable stiffness and cell anchorage: validation of its feasibility in modulating sonic hedgehog signaling pathway physically, *Macromol. Mater. Eng.* (2020) 305.
- [25] M.J. Carvell, P.J. Marsh, S.J. Persaud, P.M. Jones, E-cadherin interactions regulate β -cell proliferation in islet-like structures, *Cell. Physiol. Biochem.* 20 (2007) 617–626.
- [26] M. Olbrot, J. Rud, L.G. Moss, A. Sharma, Identification of β -cell-specific insulin gene transcription factor RIPE3b1 as mammalian MafA, *Proc. Natl. Acad. Sci. U. S. A.* 99 (2002) 6737–6742.
- [27] S. Aramata, S.I. Han, K. Yasuda, K. Kataoka, Synergistic activation of the insulin gene promoter by the β -cell enriched transcription factors MafA, Beta2, and Pdx1, *Biochim. Biophys. Acta* 1730 (2005) 41–46.
- [28] F.J. Naya, H.P. Huang, Y. Qiu, H. Mutoh, F.J. DeMayo, A.B. Leiter, et al., Diabetes, defective pancreatic morphogenesis, and abnormal enteroendocrine differentiation in β ETAR/neuroD-deficient mice, *Genes Dev.* 11 (1997) 2323–2334.
- [29] B. Coste, J. Mathur, M. Schmidt, T.J. Earley, S. Ranade, M.J. Petrus, et al., Piezo1 and Piezo2 are essential components of distinct mechanically activated cation channels, *Science* 330 (2010) 55–60.
- [30] V. Deivasikamani, S. Dhayalan, Y. Abudushalamu, R. Mughal, A. Visnagri, K. Cuthbertson, et al., Piezo1 channel activation mimics high glucose as a stimulator of insulin release, *Sci. Rep.* 9 (2019) 16876.
- [31] T.U. Greiner, G. Kesavan, A. Ståhlberg, H. Semb, Rac1 regulates pancreatic islet morphogenesis, *BMC Dev. Biol.* 9 (2009) 2.
- [32] S. Asahara, Y. Shibutani, K. Teruyama, H.Y. Inoue, Y. Kawada, H. Etoh, et al., Ras-related C3 botulinum toxin substrate 1 (Rac1) regulates glucose-stimulated insulin secretion via modulation of F-actin, *Diabetologia* 56 (2013) 1088–1097.
- [33] A. Kowluru, Friendly, and not so friendly, roles of Rac1 in islet β -cell function: Lessons learnt from pharmacological and molecular biological approaches, *Biochem. Pharmacol.* 81 (2011) 965–975.
- [34] *Nat. Commun.* 6 (2015). Article number: 6365.
- [35] A.C. Hauge-Evans, P.E. Squires, S.J. Persaud, P.M. Jones, Pancreatic β -cell-to- β -cell interactions are required for integrated responses to nutrient stimuli: enhanced Ca^{2+} and insulin secretory responses of MIN6 pseudoislets, *Diabetes* 48 (1999) 1402–1408.
- [36] M.J. Luther, A. Hauge-Evans, K.L. Souza, A. Jörns, S. Lenzen, S.J. Persaud, et al., MIN6 β -cell- β -cell interactions influence insulin secretory responses to nutrients and non-nutrients, *Biochem. Biophys. Res. Commun.* 343 (2006) 99–104.
- [37] O. Naujok, Y. Bandou, Y. Shikama, M. Funaki, S. Lenzen, Effect of substrate rigidity in tissue culture on the function of insulin-secreting INS-1E cells, *J Tissue Eng Regen Med* 11 (2017) 58–65.
- [38] Z.Q. Feng, X. Chu, N.P. Huang, T. Wang, Y. Wang, X. Shi, et al., The effect of nanofibrous galactosylated chitosan scaffolds on the formation of rat primary hepatocyte aggregates and the maintenance of liver function, *Biomaterials* 30 (2009) 2753–2763.

- [39] D. Wang, D. Cheng, Y. Guan, Y. Zhang, Thermoreversible hydrogel for in situ generation and release of HepG2 spheroids, *Biomacromolecules* 12 (2011) 578–584.
- [40] E. Maillard, M.C. Sencier, A. Langlois, W. Bietiger, M. Krafft, M. Pinget, et al., Extracellular matrix proteins involved in pseudoislets formation, *Islets* 1 (2009) 232–241.
- [41] A.R. Leite, M.L. Corrêa-Giannella, M.L. Dagli, M.A. Fortes, V.M. Vegas, D. Giannella-Neto, Fibronectin and laminin induce expression of islet cell markers in hepatic oval cells in culture, *Cell Tissue Res.* 327 (2007) 529–537.
- [42] P.O. Carlsson, Influence of microenvironment on engraftment of transplanted β -cells, *Ups. J. Med. Sci.* 116 (2011) 1–7.
- [43] G.E. Bauer, J. Balsamo, J. Lilien, Cadherin-mediated adhesion in pancreatic islet cells is modulated by a cell surface N-acetylgalactosaminylphosphotransferase, *J. Cell Sci.* 103 (Pt 4) (1992) 1235–1241.
- [44] V. Cirulli, Cadherins in islet β -cells: more than meets the eye, *Diabetes* 64 (2015) 709–711.
- [45] G. Parnaud, C. Gonelle-Gispert, P. Morel, L. Giovannoni, Y.D. Muller, R. Meier, et al., Cadherin engagement protects human β -cells from apoptosis, *Endocrinology* 152 (2011) 4601–4609.
- [46] A.D. Mendelsohn, C. Nyitray, M. Sena, T.A. Desai, Size-controlled insulin-secreting cell clusters, *Acta Biomater.* 8 (2012) 4278–4284.
- [47] A. Chowdhury, O. Dyachok, A. Tengholm, S. Sandler, P. Bergsten, Functional differences between aggregated and dispersed insulin-producing cells, *Diabetologia* 56 (2013) 1557–1568.
- [48] S. Lenzen, Signal recognition enzyme for glucose-induced insulin secretion, in: P. R. Flatt (Ed.), *Nutrient Regulation of Insulin Secretion*, 1992, pp. 101–125.
- [49] R. Barrientos, S. Baltrusch, S. Sigrist, G. Legeay, A. Belcourt, S. Lenzen, Kinetics of insulin secretion from MIN6 pseudoislets after encapsulation in a prototype device of a bioartificial pancreas, *Horm. Metab. Res.* 41 (2009) 5–9.
- [50] C. Kelly, H. Guo, J.T. McCluskey, P.R. Flatt, N.H. McClenaghan, Comparison of insulin release from MIN6 pseudoislets and pancreatic islets of Langerhans reveals importance of homotypic cell interactions, *Pancreas* 39 (2010) 1016–1023.
- [51] U. Ahlgren, J. Jonsson, L. Jonsson, K. Simu, H. Edlund, beta-cell-specific inactivation of the mouse *Ipfl/Pdx1* gene results in loss of the beta-cell phenotype and maturity onset diabetes, *Genes Dev.* 12 (1998) 1763–1768.
- [52] M. Brissova, M. Shiota, W.E. Nicholson, M. Gannon, S.M. Knobel, D.W. Piston, et al., Reduction in pancreatic transcription factor PDX-1 impairs glucose-stimulated insulin secretion, *J. Biol. Chem.* 277 (2002) 11225–11232.
- [53] A. Niknamasl, S.N. Ostad, M. Soleimani, M. Azami, M.K. Salmani, N. Lotfikhahshai, et al., A new approach for pancreatic tissue engineering: human endometrial stem cells encapsulated in fibrin gel can differentiate to pancreatic islet beta-cell, *Cell Biol. Int.* 38 (2014) 1174–1182.
- [54] J. Liu, S. Liu, Y. Chen, X. Zhao, Y. Lu, J. Cheng, Functionalized self-assembling peptide improves INS-1 β -cell function and proliferation via the integrin/FAK/ERK/cyclin pathway, *Int. J. Nanomed.* 10 (2015) 3519–3531.
- [55] R. Veluthakal, H. Kaur, M. Goalstone, A. Kowluru, Dominant-negative alpha-subunit of farnesyl- and geranyltransferase inhibits glucose-stimulated, but not KCl-stimulated, insulin secretion in INS 832/13 cells, *Diabetes* 56 (2007) 204–210.
- [56] J. Li, R. Luo, A. Kowluru, G. Li, Novel regulation by Rac1 of glucose- and forskolin-induced insulin secretion in INS-1 beta-cells, *Am. J. Physiol. Endocrinol. Metab.* 286 (2004) E818–E827.
- [57] A. Kowluru, Inappropriate movement of Rac1 contributes to glucotoxicity of the islet β -cell, *Cell Cycle* 16 (2017) 1387–1388.
- [58] T.B. Murdoch, D. McGhee-Wilson, A.M. Shapiro, J.R. Lakey, Methods of human islet culture for transplantation, *Cell Transplant.* 13 (2004) 605–617.
- [59] D.W. Fraga, O. Sabek, D.K. Hathaway, A.O. Gaber, A comparison of media supplement methods for the extended culture of human islet tissue, *Transplantation* 65 (1998) 1060–1066.